Electronic Thermal Conductivity of Superconducting Thin Films of Indium-Manganese Alloys*†

Allan W. Bjerkaas,‡ D. M. Ginsberg, and B. J. Mrstik
Department of Physics and Materials Research Laboratory,
University of Illinois, Urbana, Illinois 61801
(Received 24 September 1971)

The transition temperature T_c and the thermal conductivity of thin films of superconducting indium and indium-manganese alloys have been measured at temperatures from 1.2 to 4.2 K. The films contained 0.0–0.0567 at.% manganese. They were quench condensed on thin substrates at 4 K, and were kept below 5 K throughout the measurements. The dependence of T_c on manganese concentration is in excellent accord with the theory of Abrikosov and Gor'kov. However, the thermal-conductivity data are in systematic disagreement with the theory of Ambegaokar and Griffin and of Bennemann. This observation is related to discrepancies with theory which have been seen in the results of other experiments on the effect of transition-element magnetic impurities. Some approximations in the theory are listed which may account for the difficulty.

I. INTRODUCTION

Since the early work of Buckel and Hilsch[1] and of Matthias *et al.*,[2,3] it has become well known that the superconducting transition temperature of a metal can be sharply depressed by the electronic spins of impurity atoms with localized magnetic moments. The theory of this effect and the related effects on other superconducting properties was developed by Abrikosov and Gor'kov[4] and by Skalski *et al.*[5] There has now been a great deal of further theoretical and experimental work.[6,7] The far-infrared and tunneling experiments of Reif and co-workers[8,9] indicated that the theories correctly describe the behavior of superconductors with rare-earth impurity spins, but do not apply very well to superconductors with transition-element impurity spins. Similarly, thermal-conductivity measurements by Finnemore and co-workers[10,11] indicate that the theory of Ambegaokar and Griffin[12] and of Bennemann[13] is reasonably well satisfied for rare-earth impurity spins, but the data reported here on samples with transition-element impurity spins show a marked and systematic disagreement with the theory.

Our measurements have been performed on thin-film samples for two reasons. First, by producing the films by quench condensation from the vapor onto a very cold substrate, one can form a homogeneous alloy with a much higher concentration of transition-element impurity than for alloys formed at or above room temperature.[14] Second, because the phonon mean free path is very short in thin films, especially those which have been quench condensed, the phonon contribution to the thermal conductivity is negligible compared with the electronic contribution, so the desired electronic thermal conductivity is directly measured.[15,16] Thus, we avoid the uncertainties which would stem from a subtraction of the phonon contribution from the total thermal conductivity.

We have investigated samples of indium with various amounts of manganese. We chose indium, a rather weak-coupling superconductor which is not a transition element, for theoretical simplicity. It was already known that for quench-condensed films the manganese impurity atoms sharply depress the transition temperature,[14] indicating the presence of localized magnetic moments, although this is not the case for bulk samples of indium-manganese alloys.[17,18] To obtain homogeneous samples, many small pieces of the alloy were flash evaporated[19] from a hot filament onto the substrate. Sample homogeneity was also favored by the fact that indium and manganese have nearly the same vapor pressure at elevated temperatures.[20]

The sample film was condensed onto a circular piece of thin Kapton-H film.[21] This substrate was directly cooled to 4 K or below by liquid helium on the reverse side. The low temperature of the substrate promoted uniformity of film thickness[19] as well as of composition. During the measurements of thermal conductivity, the liquid helium was removed and the sample was cooled only from its edges by helium in another tank. To avoid precipitation of the manganese the sample was never warmed up above 5 K until the measurements were completed.

II. EXPERIMENTAL PROCEDURES

A. Cryostat

The cryostat used in this investigation was produced by adding a third liquid-helium tank to one used for prior work.[22] This third liquid-helium tank was the sample holder; it had a bottom which

was made of Kapton-H film, 5×10^{-3} in. thick, on the lower side of which the sample film was produced, as shown in Fig. 1. The two carbon-resistance thermometers attached to the substrate were glued on its upper side with GE 7031 varnish.[23] (The vacuum seal between the substrate and the rest of the tank, to which it was clamped, was a very thin layer of silicone rubber adhesive.[24]) One of the other two liquid-helium tanks cooled a 4-K heat shield; the other cooled the sample holder and the sample to various temperatures for the thermal-conductivity measurements, during which the sample holder was evacuated. Standard techniques of automatic pressure regulation of the helium bath and electronic regulation were used for temperature control. The liquid-nitrogen tank and 77 K heat shield were utilized throughout the experiment, of course.

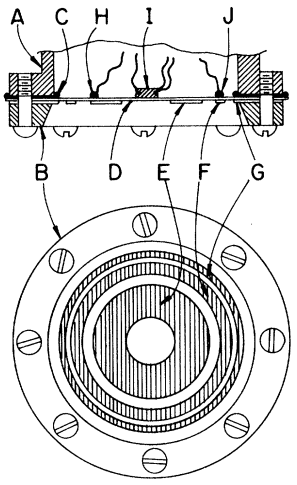

FIG. 1. Vertical cross section and bottom view of the sample and associated equipment: A, sample holder; B, clamping flange; C, rubber adhesive D, Kapton-H film substrate; E, inner silver isotherm; F, middle silver isotherm; G, outer silver isotherm; H, inner thermometer; I, sample heater; J, outer thermometer.

B. Sample Preparation

Each sample was produced as follows. To make a 2 at.% master alloy, appropriate quantities of 99.99% pure manganese and 99.999% pure indium were cleaned, weighed, and placed in a Pyrex tube. This tube had been cleaned and then outgassed at 500 °C. The tube and its contents were evacuated to a pressure less than 10^{-6} Torr, and the indium was then melted to drive off dissolved gases. The part of the evacuated tube containing the metals was then sealed off, placed in an induction coil, and heated to a dull red glow for 30 min to dissolve the manganese and stir the alloy electromagnetically. The tube was then cooled in a stream of compressed air and broken open. Any glass sticking to the alloy ingot was removed with hydrofluoric acid. The more dilute alloys were made in the same way by combining pieces of the master alloy with indium. The ingot was stored under an atmosphere of helium gas until it was used.

A piece of the ingot was folded and rolled 80 times to help ensure a uniform composition. Then pellets $0.5\times1.0\times1.0$ mm in size were cut from the resulting slab. The composition of the remaining part of the slab was determined by flame-emission spectroscopy.

In the cryostat, the pellets were flash evaporated one at a time from a hot tungsten filament[25] onto the cold substrate. As the pellets were fed to the filament by a conveyer belt, the evaporation of each pellet and the condensation of part of it onto the substrate was accompanied by a rise in the substrate temperature from about 1.2 to 3.5 K, as indicated by one of the carbon-resistance thermometers attached to the substrate. The pressure in the cryostat remained below 10^{-6} Torr throughout this procedure. Each piece of the alloy required 3–5 sec to evaporate from the filament. The filament was allowed to become white hot again between the evaporation of successive pellets; this required 5–10 sec each time. A total time of about 5 min was required to evaporate all of the pellets for a given sample. Carefully fitted shutters in heat shields were then closed to keep radiation from entering the holes through which the atoms had passed on their way from the filament to the substrate.

C. Film Geometry and Thermal-Conductivity Measurements

As shown in Fig. 1 the substrate was circular; its diameter was 2 in. A heater in the center was made of bifilarly wound wire attached to a cylindrical copper post which was glued to the upper surface of the substrate with GE 7031. With heat flowing radially outward from the heater to the edge of the sample, two carbon-resistance thermometers, similarly attached to the substrate's upper surface, measured the temperature drop between an inner and an outer radius. To prevent these thermometers from destroying the circular symmetry, we had previously deposited circular silver rings on the substrate's lower side to act as isotherms. A third silver ring at the outer edge of the sample ensured thermal contact between the sample film and the flange which clamped the substrate to the sample holder. These silver rings were 15 000 Å thick, and had a thermal conductivity of 1.11 W/cm K at 4 K. Each carbon resistor attached to the substrate was a $\frac{1}{8}$-W 150-Ω IRC resistor, with one side ground down to expose the carbon core to improve the thermal contact. The flattened side was glued to the sub-

strate. A length of each thermometer lead was also glued to the substrate above the appropriate isotherm so heat flowing in through the lead would not heat the thermometer above the temperature of the substrate. These leads were manganin wires, each 4 in. long and 0.002 in. in diameter. They were also thermally anchored directly to the sample holder. During each run, the thermometers were calibrated on the T_{58} scale by using the sample holder as a helium-vapor-pressure bulb thermometer. Random errors lead to an uncertainty of ± 0.3 mK in the temperature values, in additon to the uncertainties in the temperature scale.

During each thermal-conductance measurement a dc current passing through the heater and a series standard resistor generated voltages which were measured potentiometrically. Reversal of the current permitted a check to assure that thermoelectric voltages were not interfering significantly. For determining the heater voltage, one of the voltage leads was connected to a current lead right at the heater, and the other voltage lead was connected to the other current lead at the thermal sink. This automatically took into account the Joule heat generated in the current leads,[26] approximately half of which flowed into the sample and about half of which flowed into the thermal sink. The heater power was determined to an accuracy of 0.01%.

An ac Wheatstone bridge and lock-in amplifier were used to measure the resistances of the resistance thermometers, in each of which the power dissipation was kept below 4×10^{-9} W. The temperature drop between the inner two isotherms was measured to an accuracy of about 0.2%.

For each sample temperature the background temperature drop between the isotherms was measured with the heater current turned off. (This background temperature drop was 5–15 mK, corresponding to a heat leak of 0.1–0.5 μW.) The heater current was then turned on and adjusted to produce an additional temperature drop of about 10 mK; this required a heater power of 0.2–0.9 μW. The new temperature drop was then measured. The acquisition of each data point required a time on the order of $1\frac{1}{2}$ h. Most of this time was taken up in waiting for thermal equilibrium while controlling the sample holder's temperature to within 10 μK or less.

The differential equation which governs the steady-state flow of heat in a sample with circular symmetry is

$$\frac{dQ}{dt} = -2\pi r D K(T)\frac{dT}{dr} \quad , \tag{1}$$

where dQ/dt is the power flowing in the radial direction across a circle of radius r, D is the sample thickness, $K(T)$ is the thermal conductivity, and T is the temperature. (Radiative cooling was negligible.) To first order, $K(T)$ could be determined by setting dT and dr in Eq. (1) equal to the temperature drop between the inner two isotherms and the distance between them, respectively. We have used a slightly more accurate method which consists of fitting a power-series expression for $K(T)$ to the data.[27] The lowest-order correction from the variation of $K(T)$ between the temperatures of the two isotherms was about 0.5%; higher-order corrections were negligible. The background temperature drop from heat leaks, determined as described above, was subtracted from the data, of course. The thermal conductance of the empty cell could be determined before the sample film was condensed onto the substrate, so the thermal conductance of the sample could be found by subtraction. This measurement of the empty cell's thermal conductance was made for two samples. The results agreed to within experimental error, so the measurement was not performed on the other samples. The thermal conductances of the sample films varied from about 5% of the total thermal conductance at 1.2 K to about 20–50% of the total at 4.2 K, depending on film thickness and composition.

The important results which we report are in the form of a ratio K_s/K_n of the thermal conductivity in the superconducting state to that in the normal state. In finding this ratio it was not necessary to know the film thickness. Nevertheless, we determined the thickness D of each sample, mainly to permit us to estimate the electron mean free path. The thickness determinations were made by multiple-beam interferometry[28,29] on a separate sample, condensed onto a cover glass at the same time as the sample was produced. This substrate was attached to the edge of the sample holder, and was cooled by it. We will present thickness values later, together with indicated uncertainties corresponding to 1 standard deviation, determined by multiple measurements.

Helmholtz coils and saddle-shaped coils[30] outside of the cryostat canceled the total ambient magnetic field to within 10 mG. The coils were inadequate to drive the sample into the normal state. Therefore, the normal-state thermal conductivity K_n was obtained by interpolating between measurements above the transition temperature T_c and zero thermal conductivity at absolute zero. We used a linear interpolation, both because this is expected to fit the data in the impurity-limited conduction condition at these low temperatures, and because the measured thermal conductivity actually was proportional to the temperature above T_c. The electron mean free path l was estimated from K_n by using the Lorenz number to obtain the

TABLE I. Manganese concentration, transition temperature, resistive-transition width, film thickness, B (defined by $1/K_N = B/T$), and electron mean free path for the sample films.

Sample	$10^4 n$ (at.%) (prepared)	$10^4 n$ (at.%) (chem. anal.)	T_c (K)	ΔT_c (mK)	D (Å)	B (cm K^2/W)	l (Å)
1	0	0	3.9800	47.5	2515 ± 30	127.2	356
2	189	160 ± 2	3.1985	33.5	1150 ± 42	184.7	245
3	284	256 ± 2	2.8290	42.0	1423 ± 48	218.1	208
4	378	315 ± 6	2.3660	37.0	877 ± 49	230.3	197
5	473	424 ± 8	1.8900	45.0	2240 ± 50	...	...
6	567	496 ± 8	<1.15	...	...	...	...
7[a]	378	317 ± 18	2.5940	45.0	1618 ± 26	131.5	344
8[b]	378	334 ± 18	2.5665	34.5	1440 ± 44	154.5	293
9[c]	424	418 ± 6	1.7405	109.1	1190 ± 26	246.1	184

[a]Annealed.

[b]Probably annealed (see text).

[c]Composition uncertain (see text).

residual resistivity ρ_0; this was then divided into the value of $\rho_0 l$, which is approximately 1110 $\mu\Omega$ cm Å for indium.[31]

D. Determination of Electrical Characteristics

By means of fine wires attached to the center and the edge of the sample, the transition temperature T_c and transition width of each sample were determined while the sample holder still had liquid helium in it. The transition width is defined as the width of the temperature interval in which the sample's electrical resistance rose from 10 to 90% of the normal-state value, and T_c is defined as the temperature at which the film's electrical resistance was one half of its normal-state value. A current of 50μA was used for these measurements, which employed a four-terminal technique. Increasing the current to 200 μA did not alter the results.

E. Determination of Sample Composition

The flame-spectroscopy chemical analyses were carried out by two chemists. One analyzed samples Nos. 2–8; the other analyzed sample No. 9 (see Table I). For each of the samples Nos. 2–8, the analysis indicated a manganese composition which was about 15 % lower than that of the ingredients which had been combined. This was presumably due to the loss of manganese during the alloy preparation. Manganese oxidizes easily, and a slag which formed on each ingot was discarded. For sample No. 9, the chemical analysis indicated a manganese composition which was 98% of the combined ingredients. Hence, its composi-

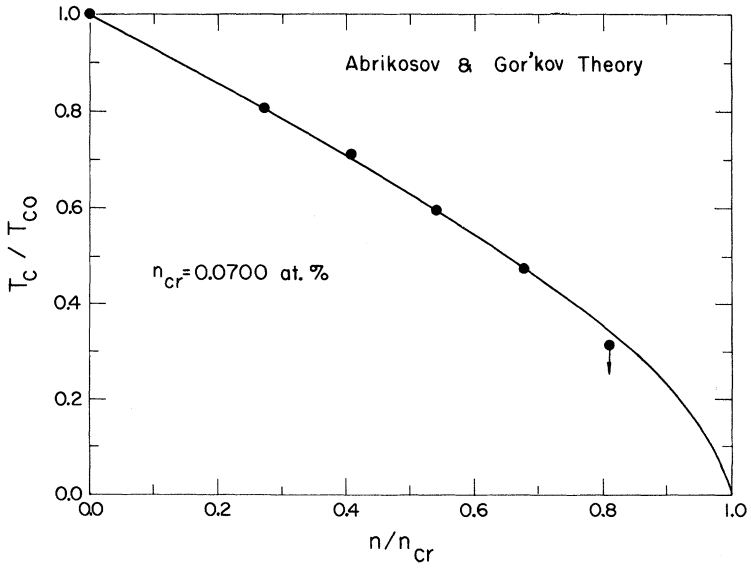

FIG. 2. Experimental and theoretical reduced transition temperature vs reduced manganese concentration. The point with the arrow indicates an upper limit; we could not reach the transition temperature of the corresponding sample.

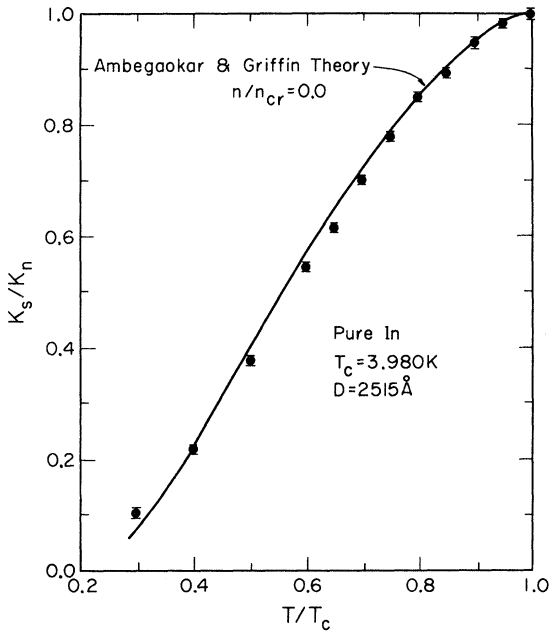

FIG. 3. Experimental and theoretical reduced thermal conductivity vs reduced temperature for sample No. 1.

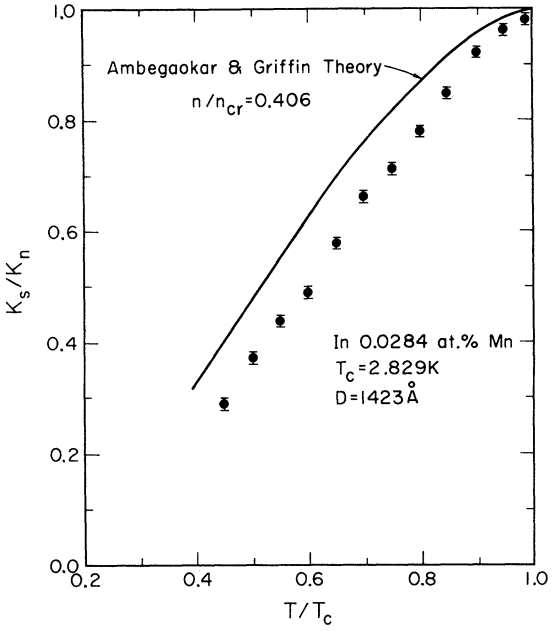

FIG. 5. Experimental and theoretical reduced thermal conductivity vs reduced temperature for sample No. 3.

tion, relative to those of the other samples, is somewhat uncertain. This sample also had a rather broad and anomalously shaped superconducting transition (109 mK wide). We have therefore not relied very much on the results from sample No. 9.

Our results are expressed in terms of the composition of the combined ingredients rather than in terms of the chemists' results, because this leads to somewhat less scatter in the plot of transition temperature vs concentration. It should be noted that the results are expressed in terms of the crit-

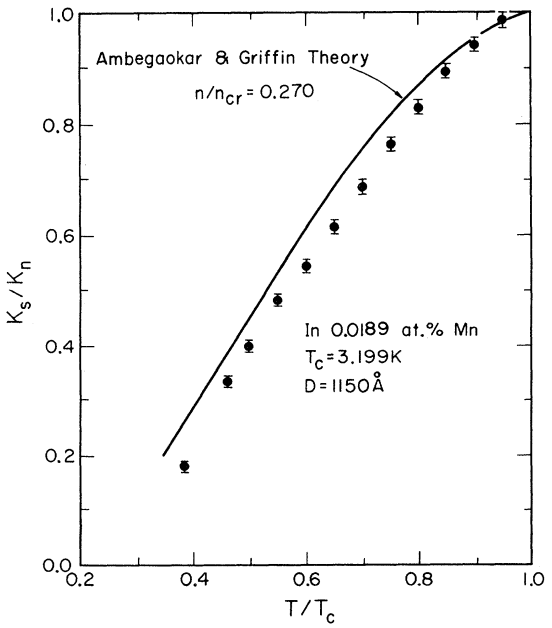

FIG. 4. Experimental and theoretical reduced thermal conductivity vs reduced temperature for sample No. 2.

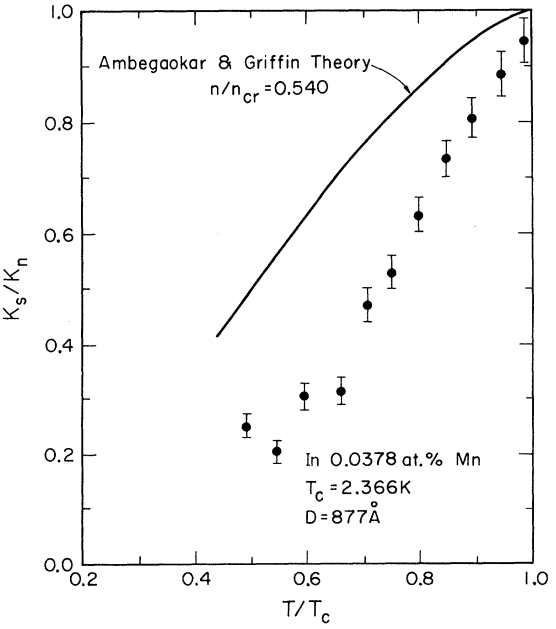

FIG. 6. Experimental and theoretical reduced thermal conductivity vs reduced temperature for sample No. 4.

ical concentration,[4] so if all of the compositions are incorrect by the same percentage, this has no effect on the test of the theory.

III. RESULTS

Some of the results are presented in Table I. The manganese concentration n as determined by the combined ingredients (in the column labeled "prepared") is thought to be more accurate, at least on a relative scale, than that indicated by chemical analysis (see Sec. IIE). The transition temperature T_c, transition width ΔT_c, film thickness D, electron mean free path l, and thermal conductivity were determined as described in Sec. II. The parameter B is defined by the relation

$$K_n = T/B \ , \tag{2}$$

where K_n is the thermal conductivity in the normal state.

Samples Nos. 7 and 8 were the first ones run. Sample No. 7 was accidentally annealed after T_c and ΔT_c were determined, but before K_n was measured. It is thought that this accounts for the low value of B for this sample. Sample No. 8, also with a low value of B, is assumed to have also been inadvertently annealed before K_n was measured. For these reasons, and because the composition of sample No. 9 was somewhat uncertain (see Sec. IIE), we will present only the results from samples Nos. 1–6 in our graphs.

In Fig. 2 the transition temperature T_c, normalized to that of the pure metal T_{co}, is plotted against concentration, normalized to the critical concentration n_{cr}. We determined n_{cr} to be 0.0700 at. % by fitting the points in Fig. 2 to the theoretical curve.[4] The fit of the points to the curve is excellent, and we take this to indicate that the impurity spins probably are not ordered[32,33] and that the Kondo effect is absent.[34] This ensures that one of the requirements of the theory with which we will compare our thermal-conductivity data is probably satisfied. The results shown in Fig. 2 agree reasonably well with those of Opitz.[14]

Figures 3–6 show the ratio of the superconducting thermal conductivity K_s to the normal-state thermal conductivity K_n as a function of temperature. The error bars in these figures represent ±1 standard deviation. It is clear that the data all fall below the theoretical curves, which have been determined by interpolation between the curves of Ambegaokar and Griffin,[12] shown in Fig. 7. The discrepancy between experiment and theory increases with increasing manganese concentration.

Figure 8 shows a plot of smooth curves drawn through the data. It can be seen that the reduced thermal conductivity of the In 0.0189 at. % Mn sample crosses the curve for pure indium, as the theory predicts. However, the crossing is at about

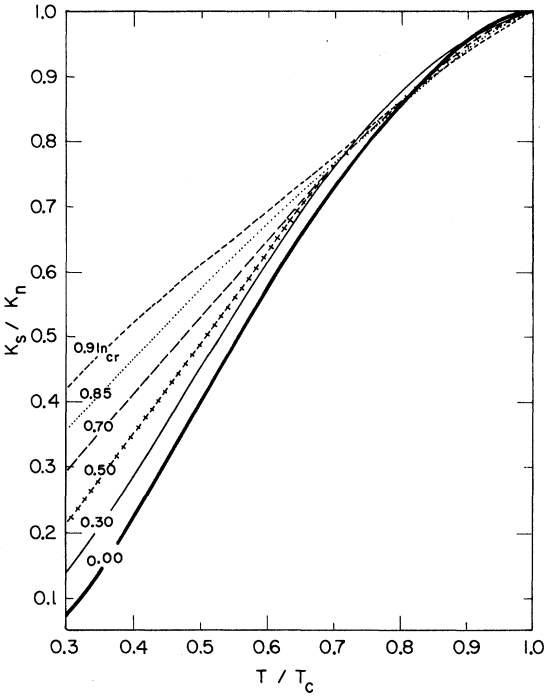

FIG. 7. Theoretical curves of reduced thermal conductivity vs reduced temperature, from Ambegaokar and Griffin (Ref. 12).

$T/T_c = 0.7$, which is lower than the theoretical crossing at 0.95. The reduced thermal conductivity of the In 0.0284 at. % Mn sample will cross the curve for pure indium at $T/T_c \lesssim 0.4$ if the data are extrapolated. This crossing is at a far lower reduced temperature than the theoretical crossing at 0.90. The reduced thermal conductivity of the In 0.0378 at. % Mn seems to be bending over to intersect the other curves, although the experimental uncertainties and scatter prevent us from being sure of this.

IV. DISCUSSION

Bennemann and Mueller[35] predicted a lower reduced thermal conductivity than expected from the theory of Ambegaokar and Griffin if the impurity spins order under certain conditions. Impurity spin ordering would thus be a possible explanation for the behavior of the thermal conductivity of our films. However, it is not a satisfying explanation, because of the lack of evidence for impurity spin ordering in the transition-temperature data (Fig. 2); spin ordering would be expected to affect the transition temperature.[32,33]

Earlier investigators have also observed discrepancies between experiment and theory for alloys of superconductors containing transition-element impurity spins. Woolf and Reif[8] observed for quench-condensed thin films that iron in indium

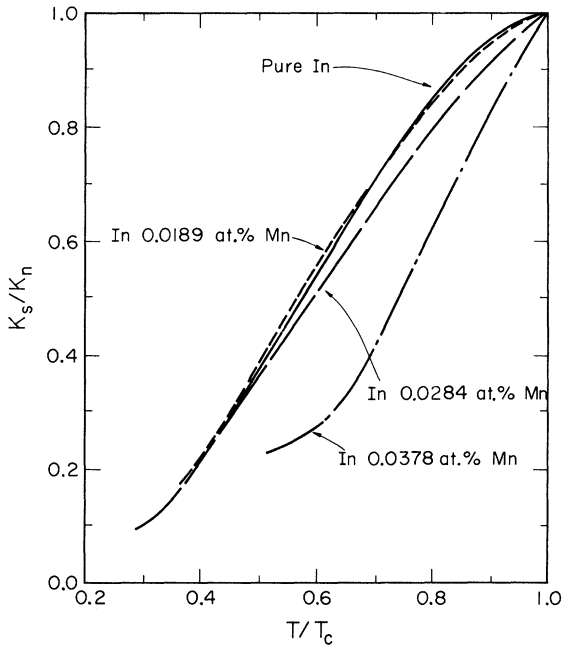

FIG. 8. Experimental reduced thermal conductivity vs reduced temperature for samples Nos. 1–4.

and manganese in lead had more pronounced effects on the energy gap than were predicted by the theory of Skalski *et al.*[5] Dick and Reif[9] observed for quench-condensed thin films that manganese in lead affects the real part σ_1 of the far-infrared electrical conductivity more drastically than predicted by the theory.[5]

Griffin[36] has pointed out some reasons why the present theories may not correctly describe the effects of transition-element impurities on superconductors. The theory of Abrikosov and Gor'kov,[4] and theories based on it,[5,12] are restricted in the following ways: (i) The impurity spins are assumed to be very well localized. This is a more accurate assumption for rare-earth impurities, with *f*-electron spins, than for transition-element impurities, with *d*-electron spins. (ii) The effect of impurity spin dynamics is neglected. (iii) Exchange scattering is treated only in lowest-order perturbation theory. (iv) The theory does not take into account the Rudermann-Kittel-Kasuya-Yosida interaction (an indirect interaction between the impurity spins caused by the conduction electrons).

Our results may indicate strong coupling between the electrons and phonons in these alloys. This could explain the discrepancy between theory and experiment.[37,38]

There needs to be more experimental work done on alloys of superconductors containing transition-element impurities. In particular, some more work should be done on indium-manganese quench-condensed films to determine definitely whether impurity spin ordering occurs. We are presently measuring the thermal conductivity of superconducting films with rare-earth impurities.

ACKNOWLEDGMENTS

One of us (A. W. B.) wishes to thank the National Science Foundation for two years of support as an NSF Trainee during the course of this work.

*Research supported in part by the National Science Foundation and in part by the Advanced Research Projects Agency under Grant No. HC-15-67-C-0221.

†Paper based in part on the Ph. D. thesis of Allan W. Bjerkaas, University of Illinois, 1971.

‡Present address: Physics Department, University of Pittsburgh, Pittsburgh, Pa. 15213.

[1]W. Buckel and R. Hilsch, Z. Physik 128, 324 (1950).

[2]B. T. Matthias, H. Suhl, and E. Corenzwit, Phys. Rev. Letters 1, 92 (1958).

[3]B. T. Matthais, H. Suhl, and E. Corenzwit, J. Phys. Chem. Solids 13, 156 (1960).

[4]A. A. Abrikosov and L. P. Gor'kov, Zh. Eksperim. i Teor. Fiz. 39, 1781 (1960) [Sov. Phys. JETP 12, 1243 (1961)].

[5]S. Skalski, O. Betbeder-Matibet, and P. R. Weiss, Phys. Rev. 136, A1500 (1964).

[6]K. Maki, in *Superconductivity*, edited by R. D. Parks (Dekker, New York, 1969), Vol 2, p. 1035.

[7]R. D. Parks, in *Superconductivity*, edited by P. R. Wallace (Gordon and Breach, New York, 1969), Vol. 2, p. 625.

[8]M. A. Woolf and F. Reif, Phys. Rev. 137, A557 (1965).

[9]G. J. Dick and F. Reif, Phys. Rev. 181, 774 (1969).

[10]R. L. Cappelletti and D. K. Finnemore, Phys. Rev. 188, 723 (1969).

[11]L. J. Williams, W. R. Decker, and D. K. Finnemore, Phys. Rev. B 2, 1287 (1970).

[12]V. Ambegaokar and A. Griffin, Phys. Rev. 137, A1151 (1965).

[13]K. H. Bennemann, Phys. Letters 14, 273 (1965). The right side of Eq. (5) should be divided by 2. It then agrees with the theory of Ambegaokar and Griffin (Ref. 12).

[14]W. Opitz, Z. Physik 141, 263 (1955).

[15]J. M. Mochel and R. D. Parks, Phys. Rev. Letters 16, 1156 (1966).

[16]J. E. Smith, Jr. and D. M. Ginsberg, Phys. Rev. 167, 345 (1968).

[17]D. L. Martin, Phys. Rev. 138, A464 (1965).

[18]G. Boato, G. Gallinaro, and C. Rizzuto, Phys. Rev. 148, 353 (1966).

[19]L. Holland, *Vacuum Deposition of Thin Films* (Chapman and Hall, London, 1966).

[20]R. E. Honig, RCA Rev. 23, 574 (1962).

[21]Kapton-H film is manufactured by E. I. DuPont De Nemours & Co., Inc., Wilmington, Del.

[22]J. S. Shier and D. M. Ginsberg, Phys. Rev. 147, 384 (1966).

[23]GE 7031 varnish is manufactured by the Insulating

Materials Department of General Electric Corp., Schenectady, N.Y.

[24]GE RTV 102 silicone adhesive is manufactured by the Silicone Products Department of General Electric Corp., Waterford, N.Y.

[25]K. Schwidtal, Z. Physik 158, 563 (1960).

[26]J. E. Neighbor, Rev. Sci. Instr. 37, 497 (1966).

[27]A. W. Bjerkaas, Ph.D. thesis (University of Illinois, 1971) (unpublished).

[28]S. Tolansky, *Multiple-Beam Interferometry of Surfaces and Films*, (Oxford U.P., New York, 1948), p. 147.

[29]H. E. Bennett and J. M. Bennett, in *Physics of Thin Films*, edited by G. Hass and R. E. Thun (Academic, New York, 1967), Vol. 4, p. 1.

[30]D. M. Ginsberg and M. J. Melchner, Rev. Sci. Instr. 41, 122 (1970).

[31]K. R. Lyall and J. F. Cochran, Phys. Rev. 159, 517 (1967).

[32]K. H. Bennemann, Phys. Rev. Letters 17, 438 (1966).

[33]J. Keller and R. Benda, J. Low Temp. Phys. 2, 141 (1970).

[34]E. Muller-Hartmann and J. Zittartz, Phys. Rev. Letters 26, 428 (1971).

[35]K. H. Bennemann and F. M. Mueller, Phys. Rev. 176, 546 (1968).

[36]A. Griffin, in *Superconductivity*, edited by P. R. Wallace (Gordon and Breach, New York, 1969), Vol. 2, p. 577.

[37]V. Ambegaokar and J. Woo, Phys. Rev. 139, A1818 (1965).

[38]W. Bergmann, Z. Physik 228, 25 (1969).

PHYSICAL REVIEW B VOLUME 5, NUMBER 3 1 FEBRUARY 1972

Thermodynamics of the Proximity Effect: Specific-Heat Jumps in Lamellar Lead-Tin Eutectic Alloys*

Jon Lechevet, J. E. Neighbor, and C. A. Shiffman
Department of Physics, Northeastern University, Boston, Massachusetts 02115
(Received 6 July 1971)

The specific-heat jump at the critical temperature has been determined as a function of D_S, the thickness of the superconducting layers. For thick layers, the jump decreases rapidly as D_S decreases, approaching a limit of about one-half the bulk value. A second jump in the specific heat (associated with the transition in the "normal" layers) decreases rapidly as the normal-layer thickness decreases, and extrapolates to zero for $D_N \approx \frac{1}{4}\mu$.

Fulde and Moormann[1] have emphasized that the jump in the specific heat of a superconductor at the critical temperature should be a very sensitive measure of the proximity effect, even in cases where the associated shift of T_c itself is small. This paper presents calorimetric data for lamellar Pb-Sn eutectic alloys which support that conclusion. The measurements also yield interesting results concerning an additional specific-heat jump which occurs in these alloys below T_c, associated with the tin-rich lamellas (the "normal" regions in the layered structure). A full description of the temperature dependence of the specific heat and a discussion of analytic procedures involved in the present work will be given in a subsequent paper.

Cylindrical specimens were prepared by directional solidification[2] of melts with the eutectic proportions[3] of 99.9999% pure lead and tin. Photomicrographs of cross sections exhibited the typical grain structure for lamellar alloys. In particular, the lamellas within each grain always lay parallel to the specimen axis, but otherwise the orientation of grains was apparently random. The average lamellar period λ was determined directly from the photographs, but surface conditions did not permit accurate measurements of individual lamellar widths. The widths of the lead-rich [superconducting (S)] and tin-rich [normal (N)] layers (D_S and D_N, respectively[4]) were calculated from the concentration of tin in the lead-rich domains (see below) together with the observed value of λ, using the equilibrium phase diagram[3] to establish D_S/D_N as a function of concentration. Nine samples were prepared, spanning the range $0.64 \leq \lambda \leq 5.5\ \mu$. Specific heats were measured using the continuous-warming technique and apparatus described earlier.[5]

Apart from D_S and D_N, the most important parameters required for comparisons with theory are the electron mean free paths, l_S and l_N, in the S and N layers. In general, lamellar specimens are not equilibrium structures, so l_S and l_N cannot be inferred from concentrations given by the alloy phase diagram. We derive the concentrations from measurements of the normal-state specific heat, using the assumption that the low-temperature lattice contribution to the molar specific heat of lead is not changed by addition of moderate amounts of the lower-mass tin solute. Values for the mean free paths (and also for slight shifts in the bulk transition temperature due to the dissolved tin) are calculated using known dependences on concentration.[6]